

Propagation of electrical signals via potassium ions in circular biofilms: An agent based computational study

Luke Peters
University of Manchester
Department of Physics and Astronomy

An analysis of electrical signalling via centrifugal potassium ion waves in circular *B.Subtilis* biofilms was completed using data produced in GRO, a computational bacterial simulator. The radial position of the wavefront was related to the time elapsed since the centralised potassium fire by fitting a parameterised sigmoid function of the form, $R = \frac{a}{(e^{-bt} + c)^d}$, producing a $\chi_{red}^2 = 0.99$. The average velocity of the potassium wavefront was related to the curvature of the wave by fitting a power law of the form, $V_{avg} = aC^{-b} + d$, where C is the wave's curvature, producing a $\chi_{red}^2 = 1.55$. The respective χ_{red}^2 values fall within 0.1% and 55% from 1.0, indicating a good and poor fit to the simulated data set respectively. The associated parameters for each fit were also calculated but provide little insight into the underlying signalling mechanism. The largest source of uncertainty on all calculated values resulted from the time resolution of data output from the simulations.

I. INTRODUCTION

A biofilm is an architectural colony of micro-organisms, usually encased in a self-produced matrix of extracellular polymeric substance (*EPS*)¹. The microbial cells in a biofilm are adherent to one-another and often to a static surface². They exhibit a high tolerance to antibiotics and disinfectants and are responsible for many clinical infections. A notable case is the formation of MRSA biofilms on hospital equipment³. However, they have useful applications in bio-remediation techniques and wastewater treatment. In order to control biofilm formation, it is important to develop an understanding of their growth and communication mechanisms.

This study is an extension to the findings of a study by Prindle *et al*⁴. The Prindle study showed that *Bacillus Subtilis* cells within a circular biofilm communicate nutrient stress via centrifugal potassium waves. This electrical signalling results in an increased protection of the biofilm from chemical attack. Hence, producing a theoretical model of this mechanism may aid advancements in the treatment of biofilm infections. Other studies imply that electrical signalling is a default communication method in bacteria. For instance, electrically mediated attraction is a process whereby extracellular potassium emitted by biofilms alters the membrane potentials of distant *Pseudomonas Aeruginosa* cells, redirecting their motility⁵.

The data used in this report was produced using the GRO framework, a programming language used in synthetic biology to prototype multi-cellular behaviors⁶. Specifically, these tools were used to simulate biofilm growth and nutrient signalling. An Agent Based computational Model *ABM* was utilised, as they are able to integrate spatially heterogeneous processes and produce the associated emergent phenomena up to an arbitrary complexity.

This report contains theoretical details of the electrical signalling mechanisms and simulation techniques utilised

in the study as well as discussions on the production of two mathematical models for signalling behaviour. The models were produced using curve-fitting procedures on simulated data sets. One model relates the radial position of the centrifugal potassium wavefront to the time since potassium firing, and the other relates the average velocity of the wave to it's curvature.

II. THEORY

The signalling studied in this report is caused by Glutamate, an amino acid required by bacteria for metabolic processes. When a central biofilm cell experiences glutamate starvation it releases potassium ions via the YugO potassium channel in it's cell membrane. This causes an increase in the extracellular potassium concentration surrounding nearby cells. The Fire-Diffuse-Fire *FDF* model states that once this concentration is above a threshold value, a neighbouring cell will itself release a certain amount of potassium. This result can be derived using the diffusion-reaction equation,

$$\frac{\partial c}{\partial t} = D\nabla^2 c - \gamma c + \alpha \sum_j \delta(\vec{r} - \vec{r}_i) \delta(t - t_i) \quad (1)$$

4

The *FDF* mechanism continues until the potassium has propagated centrifugally to the edge of the biofilm. In response, cells at the edge of the biofilm reduce their glutamate usage to reduce the stress on the central cells, increasing the biofilms protection to chemical attack,

The GRO program used in this study had growth rate parameters and a density distribution of cells selected to model a naturally formed biofilm. The program produced a nutrient signal fire in the centre of the biofilm at an arbitrary initial "fire" time $t_{fire} = 190$ (mins). This process models the release of potassium ions due to glutamate starvation. A view of the simulation at various times is shown in Fig. 1.

During the simulation, all individual cells output data to a CSV file. This data set contains the cell ID,

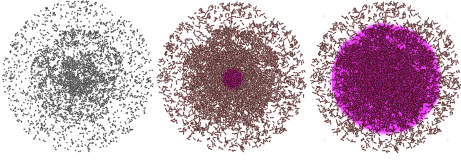


FIG. 1. A view of the simulation at various times: 9.00mins, 195.00mins and 213.00mins (left to right). The potassium concentration is shown in pink.

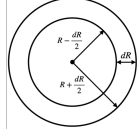


FIG. 2. Pictorial definition of the radial position procedure used throughout this report.

time(mins), potassium concentration(Arb.Units) and the X-Y coordinate of each cell. The XY coordinate axis has its origin at the centre of the biofilm hence radial distance from the centre can be calculated. An entire data set for a single simulation has around 500,000 entries.

III. DETERMINATION OF WAVEFRONT POSITION

To begin analysis of the data, a plot of the average potassium concentration per cell against time at multiple fixed radii was created. This plot is referred to as the "Potassium Profile" throughout this report. To make measurements at fixed radius, radial bands were defined such that any spatial coordinate that falls within $R \pm dR/2$ can be said to be at radius R . A representation of this technique is shown below in Fig.2.

This technique leads to an uncertainty on all radial positions of,

$$\sigma_R(step.) = \frac{dR}{2}, \quad (2)$$

Using $dR=25\mu m$, the "Potassium Profile" shown in Fig.3 was produced.

In Fig.3, a peak in the average potassium concentration is seen to propagate from low to high radii with time, this peak was used as a point of constant phase and was defined as the "position" of the centrifugal potassium wave. To reduce associated uncertainties, a smaller $dR=0.05\mu m$ was used to produce a potassium profile, and the "position" and times of the wave were plotted in Fig.4.

In Fig.4 there are multiple wave positions, occurring at the same time. This is due to the angular anisotropy of wave propagation and the large time interval, $dt=0.1$ mins, between measurements in the simulation. This time interval causes an uncertainty in the wave position's time measurements of $\sigma_T(step.) = \pm 0.05mins$. There is also the radial position uncertainty given by eq.2. These

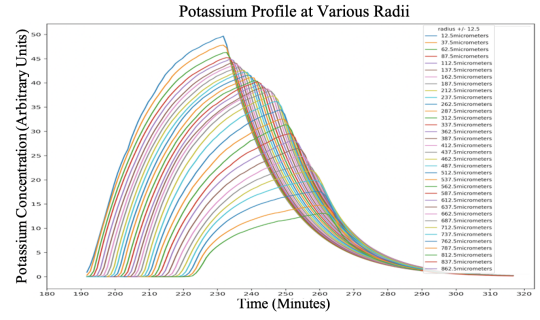


FIG. 3. A graph of the average potassium concentration per cell as a function of time at multiple fixed radii

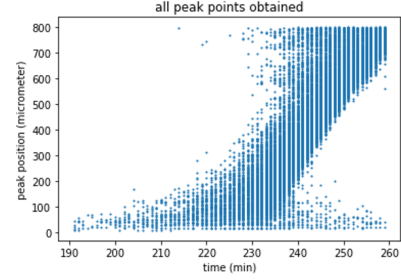


FIG. 4. A graph of all obtained peak positions from the potassium profiles using radial bands $dR=0.05\mu m$

are called (step.) uncertainties.

To account for the concurrent peaks, the mean radial position of the wave was calculated at each time, and an associated statistical uncertainty was calculated as,

$$\sigma_R(stat.) = \frac{\sigma_{sample}}{\sqrt{N}}, \quad (3)$$

where, σ_{sample} is the standard deviation about the mean and N is the number of concurrent peaks measured. Using small dR results in a large (stat.) uncertainty at large radii, using a larger dR reduces this uncertainty but results in low resolution in the small radii regime. To account for this, the final plot in Fig.5 utilises $dR=0.05\mu m$ from 0 to 31mins and $dR=0.5\mu m$ for the remainder of the time since firing. The (step.) uncertainties were neglected in final analysis as they were negligible in comparison to the (stat.) uncertainties. The resultant data was fitted to the parameterised sigmoid function,

$$R = \frac{a}{(e^{-bt} + c)^d}, \quad (4)$$

The `scipy.optimize` function in Python was used to complete a least-squares regression fit. The resultant fit is shown in Fig.5

This was followed by a plot of the average velocity as a function of Curvature= $(1/R)$, where the average velocity is defined as,

$$V_{average} = \frac{R}{t}, \quad (5)$$

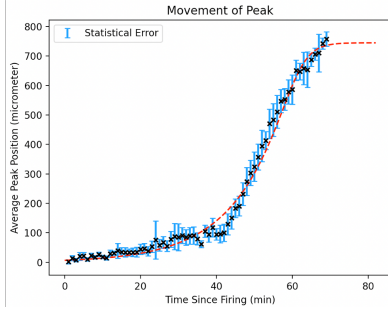


FIG. 5. A graph of average peak position against time, with the fitted sigmoid function given in eq.4

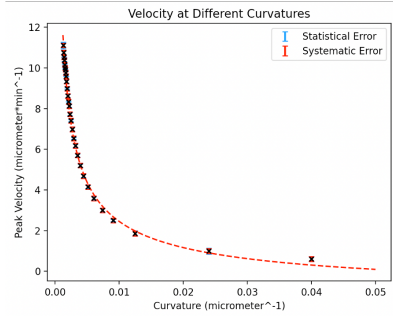


FIG. 6. A graph of average velocity, with the fitted power law function given in eq.7 for a single simulated data set

This was plotted with an associated (step.) uncertainty calculating using fractional quadrature,

$$\sigma_{V_{average}} = |V_{average}| \sqrt{\left(\frac{\sigma_R}{R}\right)^2 + \left(\frac{\sigma_t}{t}\right)^2} \quad (6)$$

and a (stat.) uncertainty on $1/R$ calculated using eq.3. Using `scipy.optimize` the resultant plot was fitted with a power law of the form,

$$V_{average} = a\left(\frac{1}{R}\right)^{-b} + c \quad (7)$$

For this fit, 6 independent simulations were completed in order to account for the stochastic nature of the ABM. This results in 6 separate fits with their own parameters, a , b and c as in eq.7, one of these plots is shown in Fig.

A weighted mean and associated uncertainty from the 6 data sets was calculated for each parameter to produce

a mean fit. The weighted mean for each parameter was calculated as,

$$X_{mean} = \frac{\sum_i X_i \frac{1}{(\sigma_{X_i})^2}}{\sum_i \frac{1}{(\sigma_{X_i})^2}} \quad (8)$$

A χ_{red}^2 was calculated for both fits using,

$$\chi_{red}^2 = \frac{\sum_{i=1}^N \left(\frac{y_i - y(x_i; a_1 \dots a_M)}{\sigma_i} \right)^2}{N - 1} \quad (9)$$

IV. RESULTS AND CONCLUSION

For the sigmoidal fit (eq.4 Fig.5), the $\chi_{red}^2=0.99$. This falls within 0.01 % of the value for an ideal fit indicating a good model. The sigmoidal fit can be explained using the FDF model. The release and accumulation of potassium ions does not happen instantaneously, hence the the peak in concentration is at a smaller radius than the most recent potassium fire. At radii near the centre, the extracellular potassium concentration only increases due to cells in front of the wave peak, and at low radii ,this increase is only due to the cells behind it. At some radius between the centre and edge there is potassium fire and diffusion occurring in front and behind the wave peak causing it to propagate faster, hence the steep gradient in Fig.5 between 100-750 μ m. The relevant parameters for this fit were calculated as $a = 6.6 \pm 0.8$, $b = 0.4 \pm 0.1$, $c = 5 \times 10^{-11} \pm 4 \times 10^{-10}$ and $d = 0.20 \pm 0.08$ where all uncertainties are statistical. Parameters a, b, c and d have % uncertainties of, 12%, 25%, 800% and 40%. These uncertainties are large due to the poor time resolution between data outputs in the simulation. A simulation that was capable of outputting data in smaller time intervals would provide a more accurate measurement of the waves radial position.

For the power law fit (eq.7 Fig.6), the $\chi_{red}^2=1.55$. This falls within 55% of the value for an ideal fit indicating a poor model. This is largely due to poor knowledge of the stochastic nature of the simulation and an inability to combine the (step.) and (stat.) errors due to their inherent correlation. The relevant parameters for this fit were calculated as $a = 0.31 \pm 0.02$, $b = 0.554 \pm 0.009$, and $c = 1.7 \pm 0.1$ where all uncertainties are statistical.

¹ H.-C. Flemming *et al.* . The eps matrix: The ‘house of biofilm cells’. *J. Bacteriol.*, 189(22).

² R. Doyle. Microbial growth in biofilms, part a. *Methods Enzymol.*, 336:1–22, 2001.

³ S.Bhattacharya *et al.* Evaluation of multidrug resistant staphylococcus aureus and their association with biofilm production in a tertiary care hospital. *J Clin Diagn Res.*, 189(16):508, 2015.

⁴ A. Prindle *et al.* Ion channels enable electrical communication in bacterial communities. *Nature*, 527(59-63), 2015.

⁵ J.Humphries. *et al.* Species-independent attraction to biofilms through electrical signaling. *Physics Letters B*, 168 (1-2), 2017.

⁶ A new improved and extended version of the multicell bacterial simulator gro.